APPLICATION NOTE

Understanding the anti-inflammatory effects of a microbiota-derived metabolite using high-content analysis and AlphaLISA technology

Key features

- High-content assay to measure IκB-α degradation
- No-wash AlphaLISA TNF quantification with as low as 5 µL of sample

Introduction

According to in *vitro, in vivo,* and clinical research, the gut microbiota postbiotic metabolite urolithin A (UroA) has intriguing biological activity. UroA is a metabolite derived from the gut-microbiome metabolism of ellagitannins.[1] These polyphenolic compounds are present in different fruits, such as berries and pomegranate. After ingestion, they are first hydrolysed and metabolised into ellagic acid, and then metabolised further into urolithins, which display enhanced bioavailability compared with their precursor.[2] UroA is specifically produced by metabotype-A individuals whose microbiota includes those microorganisms capable of producing this specific isoform, but UroA levels may also be affected by antibiotic consumption and other lifestyle factors. Accordingly, synthetic UroA has been explored as a potential anti-inflammatory, anti-oxidative, and anti-ageing, microbiota-derived small molecule.[3]

As shown by a recent study from Abdelazeem et al., UroA was able to counteract the LPS-induced IKB-α phosphorylation measured by a western blot analysis.[4] IKB-α is the natural inhibitor of NF-κB, the main transcription factor involved in inflammation. The role of IKB-α, in physiological conditions, is to restrain NF-κB in the cytosol. Once LPS is detected by TLR4, a signalling cascade leads to IκB-α phosphorylation. This event causes IKB-α to be degraded to free NF-κB and let it translocate into the nucleus, where it governs the expression of many inflammatory-related genes.[5] The authors also confirmed downregulation of IL-1β, IL-6, IL-12, TNF expression by UroA measured by qRT-PCR (versus GAPDH) and ELISA. Work from Toney and Chung also reported a significant decrease of IL-1β in UroA-treated BMDM *in vitro*.[6]

For research use only. Not for use in diagnostic procedures.

Here, we employed a strategy that combines high-content analysis and AlphaLISA cytokine detection (Figure 1) to further characterise the anti-inflammatory effect of Urolithin A on LPS-stimulated human macrophage-like cells.

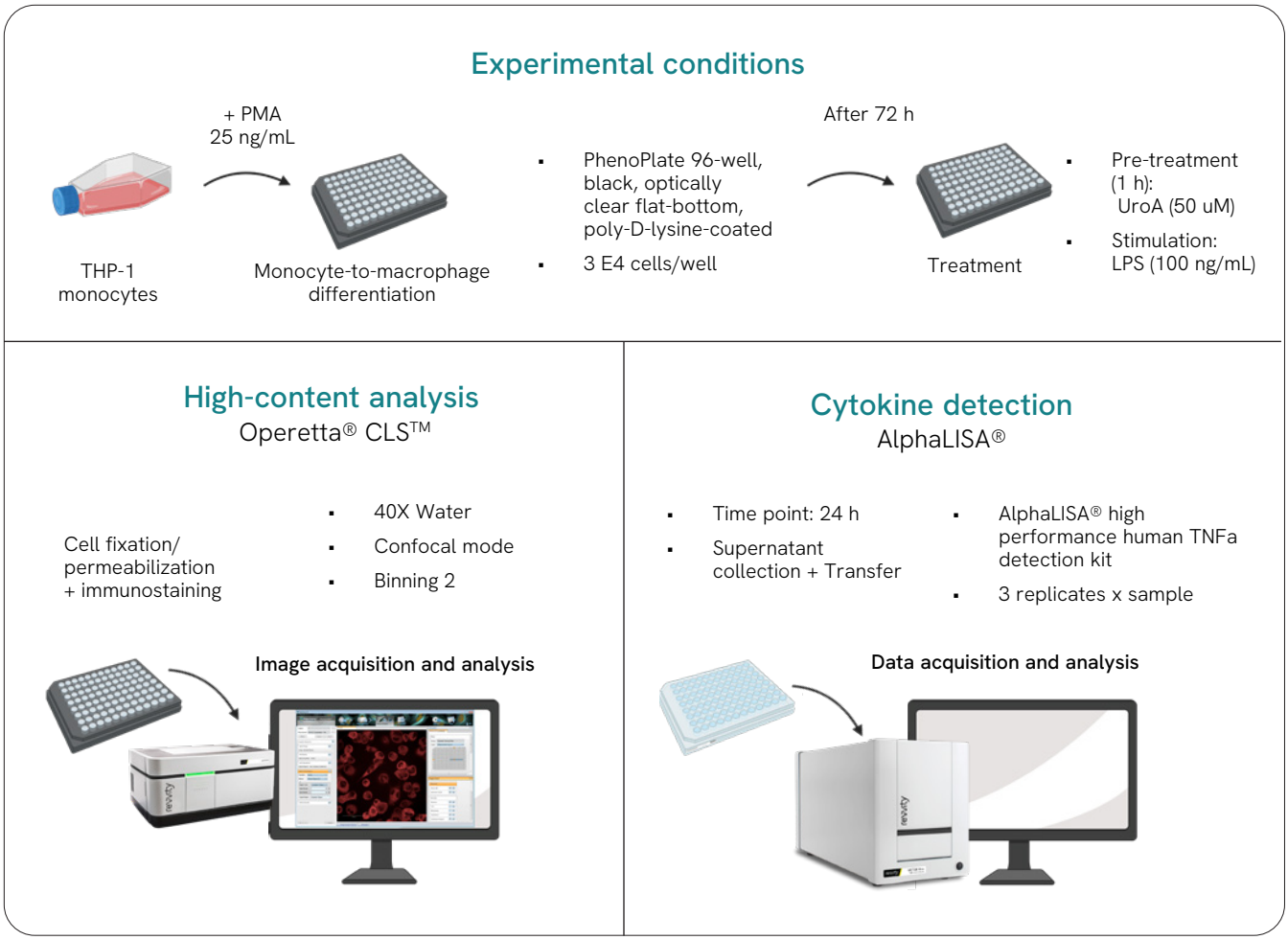

Figure 1: Experimental workflow for the evaluation of the anti-inflammatory effects of Urolithin A on macrophage-like cells. THP-1 monocytes were differentiated to macrophages by culturing them in the presence of PMA. Cells were then pre-treated with UroA or left untreated. Subsequently inflammation was triggered with LPS. For high-content analysis, cells were fixed and stained for IκB-α at various time points post LPS trigger. Cells were stained with IκBα Mouse mAb, Goat anti-mouse IgG secondary antibody, Alexa Fluor™ 647 and PhenoVue™ Hoechst 33342 nuclear stain. Imaging was performed on the Operetta® CLS™ high-content analysis system. Cytokine detection in cell supernatants was performed using a AlphaLISA High Performance TNFα assay at 24hrs post LPS trigger on a VICTOR® Nivo™ multimode microplate reader. Created with BioRender.com

Materials and methods

Table 1: List of materials, instruments, and software used in the evaluation of the anti-inflammatory effects of UroA.

Materials and instruments	Software
Cells	THP1-XBlue™ cells (Invivogen)
Growth medium	RPMI 1640 w/ L-Glutamine (Euroclone S.p.A. #ECB2000) 10% Foetal bovine serum (Euroclone S.p.A #ECS0180L) 1% Penicillin-Streptomycin solution 100X (Euroclone #ECB3001) 1% L-Glutamine 100X 200 mM (Euroclone #ECB3000)
Differentiation stimulus	Phorbol 12-myristate 13-acetate (PMA) (Invivogen #tlrl-pma)
Inflammatory stimuli	LPS E.coli O55:B5 (Sigma-Aldrich®, #L2637), LPS S.minn (S-form) (Innaxon, #IAX-100-020-M001)
Postbiotic compound	Urolithin A (Sigma-Aldrich® #SML1791)
Microplates and sealing	PhenoPlate™ 96-well, black, optically clear flat-bottom, poly-D-lysine-coated (Revvity #6055508)
Cell staining	IκBα Mouse mAb (Cell Signaling Technology, Inc. #4814) Goat anti-mouse IgG secondary antibody, Alexa Fluor™ 647 (Invitrogen #A-21235) PhenoVue™ Hoechst 33342 nuclear stain (Revvity #CP71)
Imaging instrument	Operetta® CLS™ high-content analysis system (Revvity)
Cytokine detection reagents	Human TNF-alpha DuoSet ELISA (R&D Systems, Inc. #DY210) AlphaLISA High Performance Human TNFα Detection Kit (Revvity #AL3157C)
Plate reader instrument	VICTOR® Nivo™ multimode microplate reader (Revvity)

Cell culture and monocyte-to-macrophage differentiation

THP1-XBlue™ cells (Invivogen) were cultured in Roswell Park Memorial Institute Medium (RPMI) supplemented with 10% heat-inactivated FBS, 2 mM glutamine and 100 U/mL of penicillin and streptomycin. Cells were maintained in a humidified incubator at 37° C. Cell density was maintained between 0.5 and 1 x 10^6 cells/mL by splitting cells 3 times a week. Macrophage-like cells were obtained via differentiation of THP1-XBlue™ cells by exposure to 100 ng/mL phorbol 12-myristate 13-acetate (PMA, Invivogen). Cells were seeded in 96-well plates at different densities according to the designed experiment. After 72 h of incubation with PMA, cell differentiation was assessed by optical microscope inspection.

Cell treatment

After differentiation, THP1 XBlue™ derived macrophages (TDM) were pre-treated for 1 h with 25-50 µM UroA, and then triggered with either 100 ng/mL LPS *E. coli* or LPS *S. minn.* According to the subsequent analysis, cells and/or supernatants were collected and processed (or stored) at specific time points after LPS stimulation.

Cell staining

TDM were seeded and differentiated in poly-D-lysine-coated 96-well PhenoPlates (2 x 10^4 cells/well). After differentiation, cells were pre-treated with 50 µM UroA (1 h) and then challenged with either *E. coli* or *S.minn* LPS at different time points (0-0.5-1-1.5-2-4h). The final volume was 200 µL/well. Treatment was then stopped by removing the supernatant and washing cells once with Dulbecco's Phosphate Buffered Saline (PBS) (Euroclone #ECB4053). All subsequent steps were performed at room temperature. Cells were then fixed by adding 50 µL/well of 4% paraformaldehyde (PFA) solution in PBS to each well and incubating for 10 min. Then PFA solution was aspirated and cells were washed three times by adding 200 µL/well of PBS. Permeabilization of cell membranes, to allow cytosolic protein visualisation, was achieved by adding 50 µL/well of PBS 0.1% Triton X-100 for 10 min. Cells were then washed three times as indicated before. Aspecific antibody binding was prevented by adding 50 µL of 1% BSA in PBS for 60 min. Cells were then washed three times. Immunostaining of IKB-α was performed by adding 50 µL of a 1:500 dilution of anti-IκB-α primary antibody to each well and incubating for 60 min. Cells were then washed three times, before the addition of 50 µL/well of

a 1:250 dilution of Goat anti-Mouse IgG secondary antibody, Alexa Fluor™ 647 and incubating for 60 min. After three more washes to remove the excess antibodies, nuclei were counterstained by adding 50 µL/well of a 1:5000 dilution of PhenoVue Hoechst 33342 nuclear stain to each well and incubating for 10 min. After three more wash steps, 200 µL/well of PBS were added to prevent desiccation and plates were stored at 4° C wrapped with aluminium prior to the image acquisition.

Image acquisition

PhenoPlates containing the stained cells (room temperature) were inserted into the Operetta CLS high-content analysis system. Images were acquired using the Revvity Harmony® high-content imaging and analysis software, by selecting confocal mode, 63x water immersion objective and setting binning at 2. Brightfield, Digital Phase Contrast (DPC), Alexa Fluor 647 and DAPI channel settings were adjusted individually, to obtain focused and bright images. A total of 121 (11x11) fields of view were acquired per well.

Image analysis

Images were analysed using Harmony software using a subset of building blocks as shown in Figure 2. An example *Input Image* was selected, *'Find Nuclei'* was launched, and the best-fitting algorithm was chosen to be applied on the DAPI channel to be able to count and segment each nucleus. Then, *'Find Cytoplasm'* was selected to be applied to the DPC channel in order to contour each cell cytoplasm and obtain an (image) area of interest. To exclude cells from the analysis whose cytoplasm was not imaged in its entirety, the *"Remove Border Objects"* options within the *'Select Population'* building block was applied. The intensity of the fluorescence of interest was then calculated using the *'Calculate Intensity Properties'* building block on the AlexaFluor 647 channel. Finally, the *'Select Population'* building block was applied once more to select those cells that had an intensity greater than a previously determined threshold value (from the cytosolic intensity of the non-treated cells). The complete analysis procedure was then tested for its suitability against other images from the image bulk. The final result was a numerical value for each sample that represents the average of all the acquired fields of view.

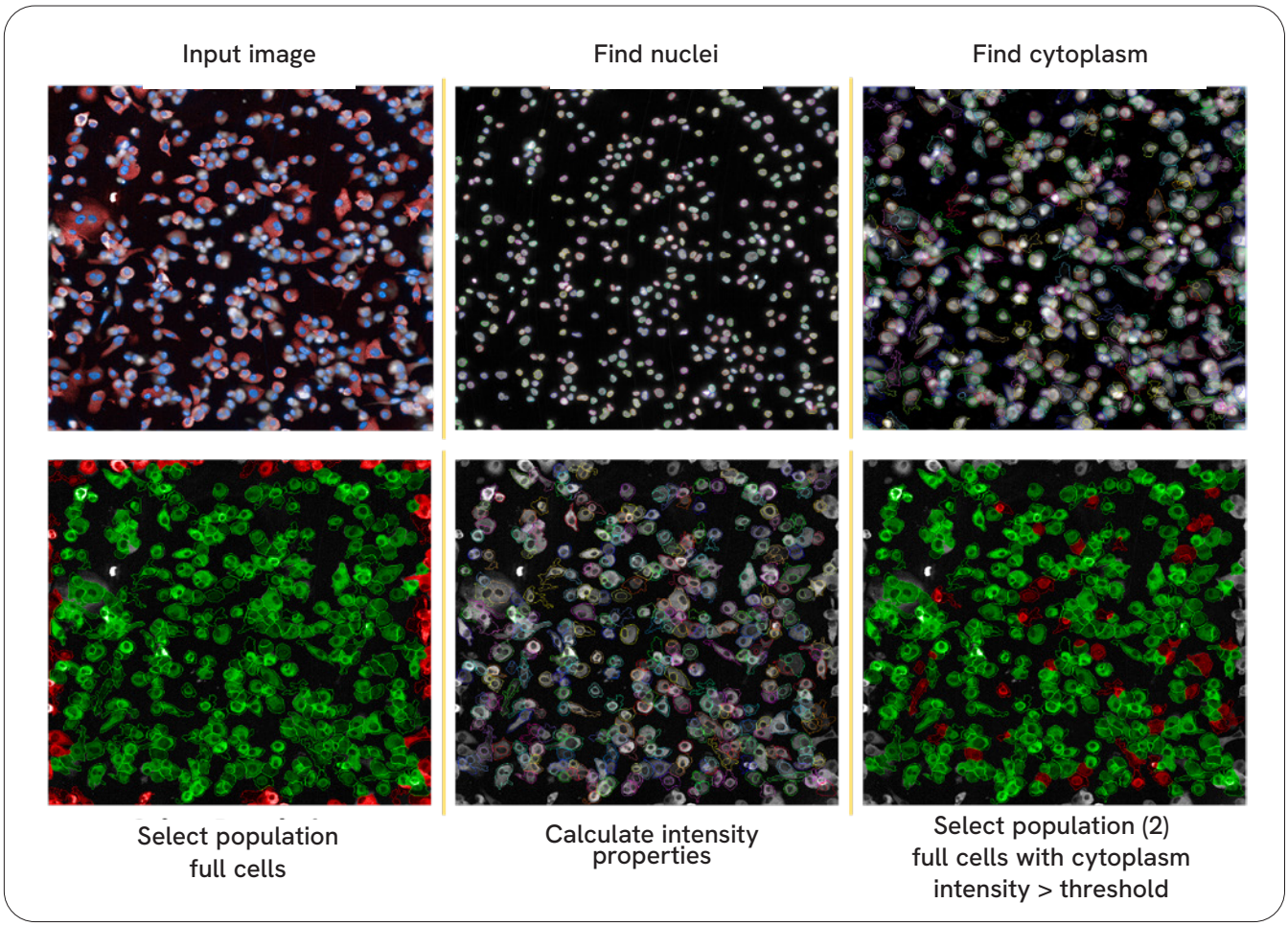

Figure 2: Setting of the image analysis sequence in Harmony software.

Numerical data were exported into an Excel spreadsheet. Calculations and subsequent data visualisation were performed using GraphPad Prism (v. 9.5.1).

Cytokine detection

TDM were seeded and differentiated in TC-treated 96-well plates (6 x 10^4 cells/well). After differentiation, cells were pre-treated with 50 µM UroA (1 h) and then challenged with either *E. coli* or *S.minn* LPS for 24 h. Cell supernatants were collected and stored at -20 °C prior to further analysis. The same samples were tested for TNF-α detection using a standard ELISA kit and the AlphaLISA High Performance Human TNFα Detection Kit, following the manufacturer's instructions.

Results and discussion

At first, it was confirmed that UroA alone does not have any effects on cell viability using an MTT colorimetric cell viability assay or on NF-κB signalling using an NF-κB inducible SEAP reporter gene assay (results not shown). A combined treatment of cells with either *E. coli* or *S. min*n LPS and UroA did also not affect cell viability (results not shown).

Effect of UroA pre-treatment on the LPS-induced IκB-α degradation

To evaluate the effect of UroA on IκB-α degradation using the Operetta CLS, THP-1 cells were exposed to PMA and seeded into poly-D-lysine-coated PhenoPlate 96-well, with optically clear flat-bottom. The optimal cell density for achieving the best cell segmentation was determined to be 3 x 10^4 cells/well. After differentiation into TDM, cells were pre-treated with UroA for 1 h and then challenged with LPS from *E. coli* or *S.minn* from 0 up to 4 h. Images corresponding to different time points post LPS administration were acquired in order to characterise the kinetics of IκB-α degradation (0-0.5-1-2-4-6). Maximum degradation of IκB-α (about -40%) was observed after 1 h post LPS exposure. Representative images for each sample corresponding to the selected time point are depicted in Figure 3. Numerical data for fluorescence intensity were obtained from the image analysis, exported and further analysed (Figure 4).

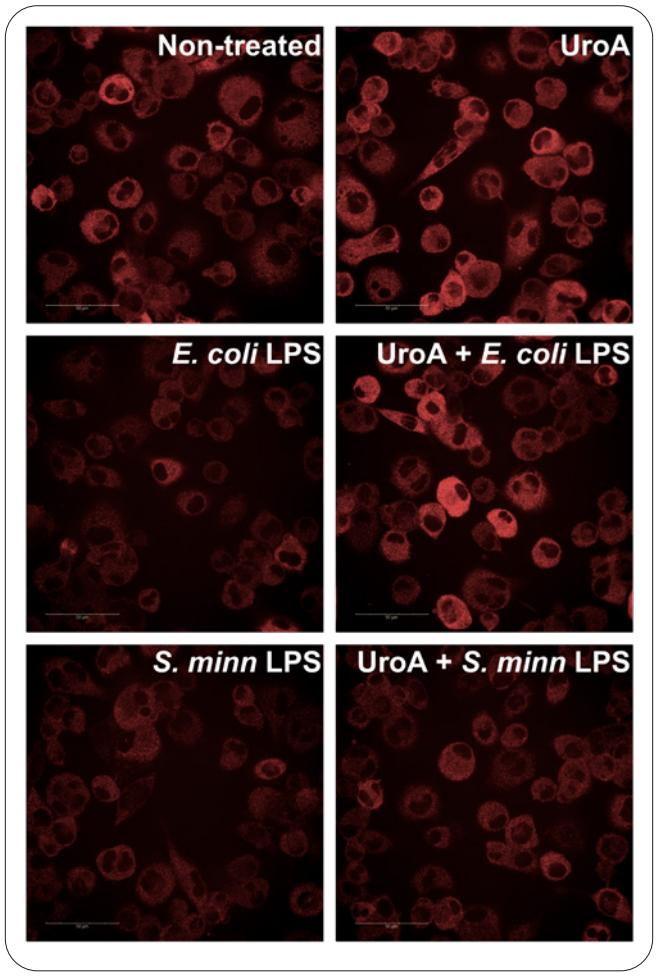

Figure 3: UroA pre-treatment slightly diminishes LPS-induced IκB-α degradation. TDM cells were pre-treated for 1 h with UroA, or left untreated. Subsequently inflammation was induced with either *E. coli* or *S. minn* LPS for 1 h. Cells were fixed and stained for IκB-α and analyzed on the Operetta CLS system.

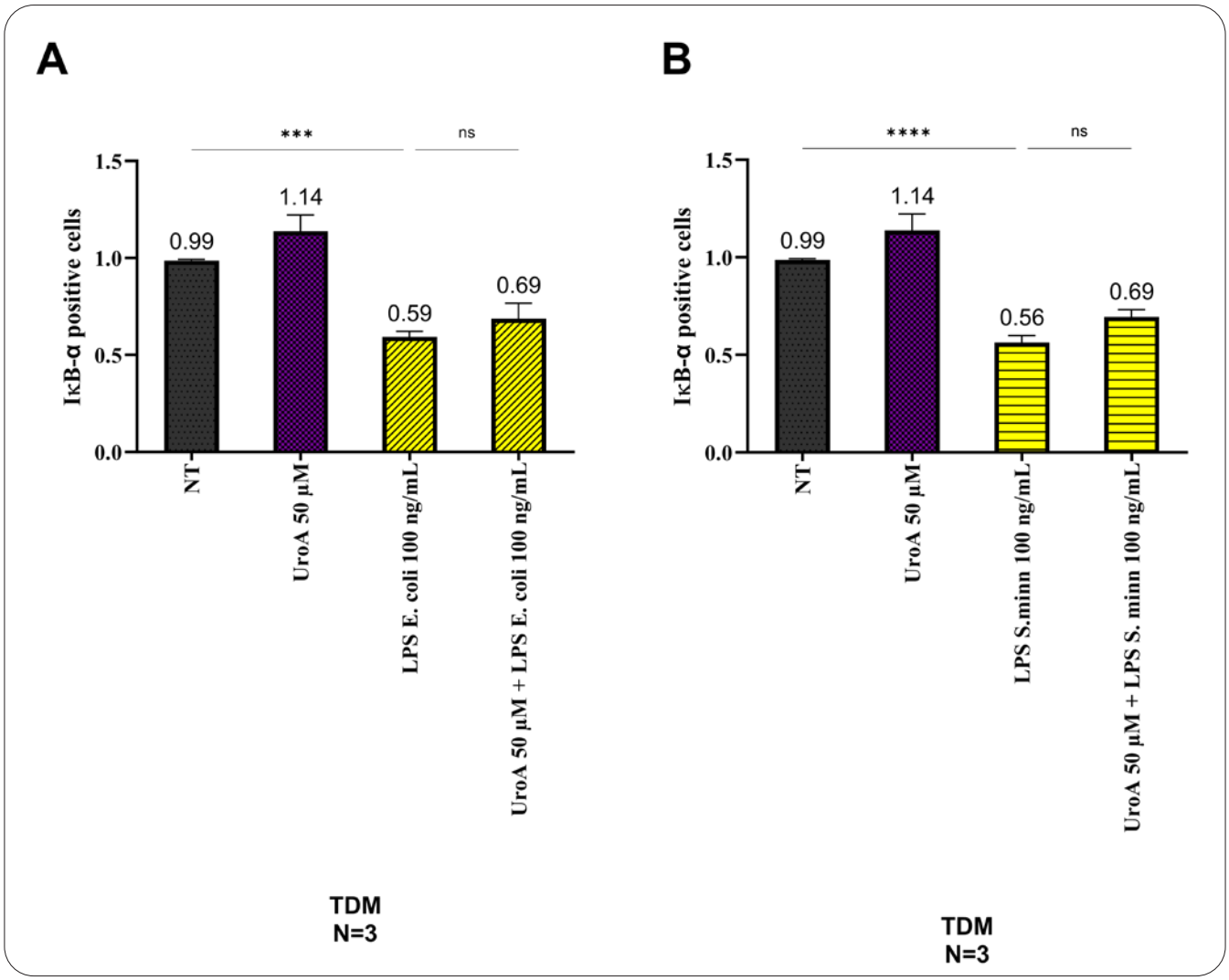

Figure 4: Quantification of IκB-α positive cells after exposure with LPS *E. coli* (A) or *S. minn* (B). In both cases TDM were treated with either UroA or LPS, or pre-treated with UroA prior to LPS exposure. (N = 3 experiments).

Untreated cells labelled for IκB-α visualisation displayed a diffuse red fluorescence in the whole cytoplasm, which reflects its physiological localisation. *E. coli* and *S. minn* LPS treatment resulted in a significant decrease in IκB-α-associated fluorescence intensity (Figure 3) demonstrating its degradation, which represents one of the necessary steps toward NF-κB activation. Statistical analysis confirmed the significance of the diminished fluorescence both in the case of *E. coli* LPS administration (Figure 4A) and *S. minn* LPS treatment (Figure 4B). UroA pre-treatment tended to inhibit LPS-induced IκB-α degradation, although this effect was not statistically significant in the case of both LPS treatments (Figure 4A and 4B).

Effect of UroA pre-treatment on the LPS-induced TNF-α secretion

In order to evaluate the effect of UroA on LPS-stimulated TNF-α release, TDM were pre-treated with 50 µM of UroA for 1 h and then exposed to LPS from *E. coli* or *S.minn* for 24 h. The resulting supernatant was then used to quantify TNF-α production using both a traditional ELISA kit and a High Performance AlphaLISA Human TNFα detection kit. In the latter, the standard curve was constructed using a 1:1 mixture of cell culture medium (RPMI) and HiBlock buffer, to decrease the medium's influence on the readings. Samples were also mixed with HiBlock buffer in a 1:1 ratio, to match the standards. This strategy was compared to using only RPMI or HiBlocK buffer and showed better performance.

In accordance with Abdelazeem et al., a significant decrease in LPS-triggered TNF-α secretion in cells pre-treated with UroA was observed (Figure 5).[4]

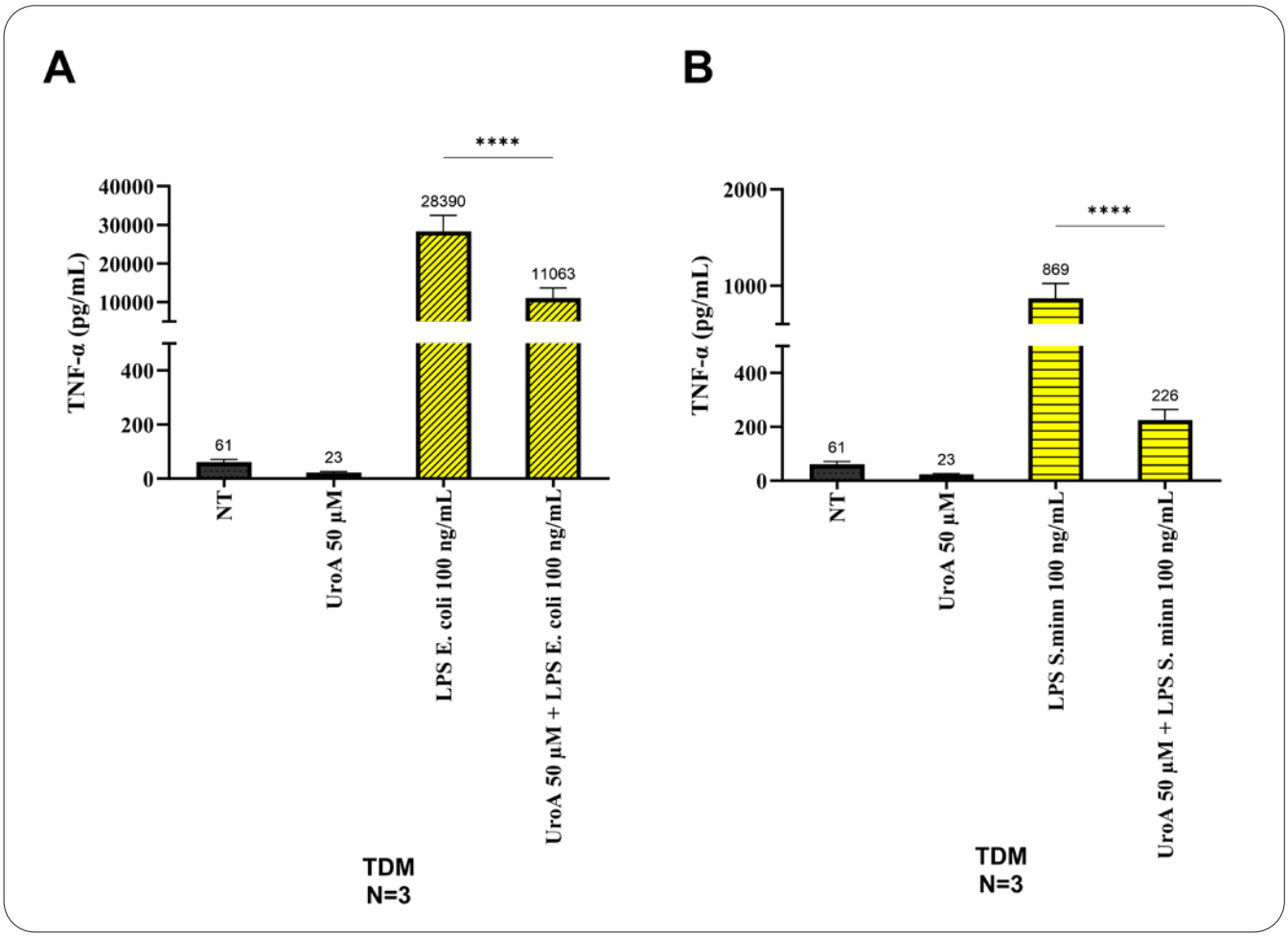

Figure 5: UroA strongly inhibits *E. coli* LPS and *S. minn* LPS induced TNF-α secretion measured by AlphaLISA. TNF-α was detected using an AlphaLISA High Performance Human TNFα Detection Kit.

Additionally, we measured TNF release into the medium using a standard ELISA kit (Figure 6) to compare results from two different methods.

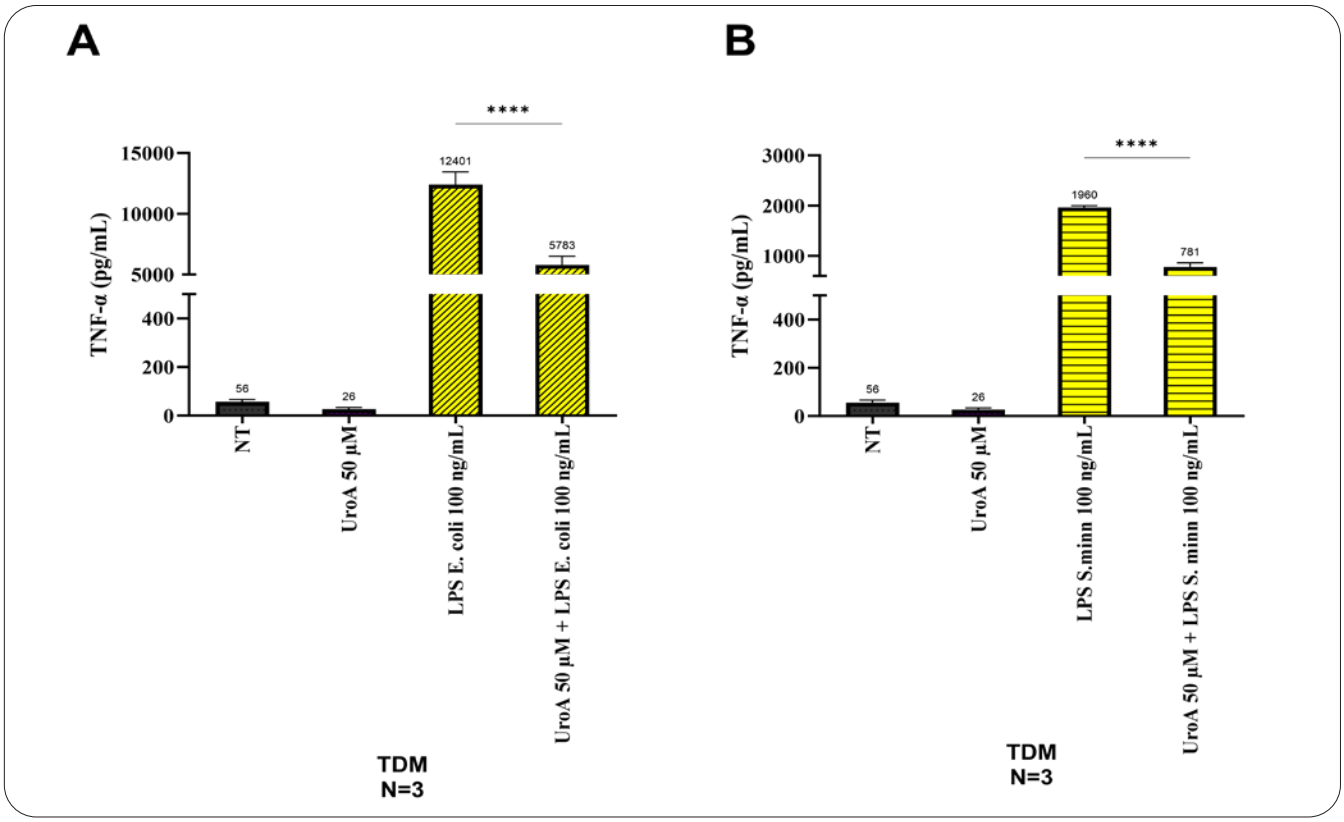

Figure 6: UroA strongly inhibits *E. coli* LPS and *S. minn* LPS induced TNF-α secretion measured by ELISA. TNF-α was detected using a standard ELISA kit.

Results showed that the inflammatory response triggered by both LPS serotypes (*E. coli* and *S. minn*) was counteracted by UroA, resulting in a dramatic decrease of TNF-α released (-53% and -60% quantified by standard ELISA, -61% and -70% in the case of the AlphaLISA, respectively). Data obtained employing the AlphaLISA kit corroborates the Operetta CLS data. A slight inhibition of IκB-α degradation by UroA pre-treatment (Figures 3 and 4) corresponds to a marked decrease in TNF secretion (Figure 5). Interestingly, we also observed decreased basal TNF levels by comparing NT cells with UroA-treated cells (in absence of LPS). These results validate the IκB-α degradation analysis performed with the Operetta CLS where UroA-treated cells showed a slightly increased (+14%) IκB-α-related fluorescence intensity located in the cytoplasm compared to NT cells.

Conclusion

Microbiota has become one of the hot topics in science not only due to their important role in maintaining homeostasis but also due to their contribution to disease when dysbiosis is present.[7] Diet has a critical role in determining gut microbiota composition and function and, indeed, dietary interventions are non-invasive and affordable approaches to re-establish gut eubiosis.[8,9] From this perspective, microbiome-derived metabolites have gained a lot of attention. These compounds have shown different disease-modulating activities. One compound in particular, UroA, has demonstrated to have a clear anti-inflammatory effect by inhibiting NF-κB signalling and decreasing the production of pro-inflammatory cytokines. Here, we showed that pre-treatment of human macrophage-like cells with 50 µM UroA resulted in diminished LPS-induced IκB-α degradation. The Operetta CLS enabled the acquisition and analysis of a large number of images, with more than a hundred fields of view per sample and per time point, in a short amount of time. Additionally, UroA pre-treatment significantly decreased the LPS-triggered TNF secretion. Our results showed that AlphaLISA data were comparable to standard ELISA data in terms of proportion among different treatments. The advantage of using a very small amount of sample (5 µL) together with the no-wash protocol makes the AlphaLISA kit a high-performance, less time-consuming approach for TNF quantification.

Taken together, these results support the hypothesis that consuming foods which contain UroA precursors may be a promising intervention strategy to reduce chronic inflammation.

References

1. Sabahi S, Homayouni Rad A, Aghebati-Maleki L, Sangtarash N, Ozma MA, Karimi A, et al. Postbiotics as the new frontier in food and pharmaceutical research. Crit Rev Food Sci Nutr. 2022 Mar 29;1–28.

2. Korczak M, Roszkowski P, Granica S, Piwowarski JP. Conjugates of urolithin A with NSAIDs, their stability, cytotoxicity, and anti-inflammatory potential. Sci Rep. 2022 Jul 8;12(1):11676.

3. Singh R, Chandrashekharappa S, Bodduluri SR, Baby BV, Hegde B, Kotla NG, et al. Enhancement of the gut barrier integrity by a microbial metabolite through the Nrf2 pathway [Internet]. Vol. 10, Nature Communications. 2019. Available from: http://dx.doi.org/10.1038/s41467-018-07859-7

4. Abdelazeem KNM, Kalo MZ, Beer-Hammer S, Lang F. The gut microbiota metabolite urolithin A inhibits NF-κB activation in LPS stimulated BMDMs. Sci Rep. 2021 Mar 29;11(1):7117.

5. Roff M, Thompson J, Rodriguez MS, Jacque JM, Baleux F, Arenzana-Seisdedos F, et al. Role of IkBα Ubiquitination in Signal-induced Activation of NF-kB in Vivo(*). J Biol Chem. 1996 Mar 29;271(13):7844–50.

6. Toney A, Chung S. Urolithin A, a Gut Metabolite, Induces Metabolic Reprogramming of Adipose Tissue by Promoting M2 Macrophage Polarization and Mitochondrial Function (OR12-02-19). Current Developments in Nutrition [Internet]. 2019 Jun [cited 2023 Feb 21];3(Suppl 1). Available from: https://www.ncbi.nlm.nih.gov/pmc/articles/PMC6573912/

7. Afzaal M, Saeed F, Shah YA, Hussain M, Rabail R, Socol CT, et al. Human gut microbiota in health and disease: Unveiling the relationship. Front Microbiol. 2022 Sep 26;13:999001.

8. Zhang P. Influence of Foods and Nutrition on the Gut Microbiome and Implications for Intestinal Health. Int J Mol Sci [Internet]. 2022 Aug 24;23(17). Available from: http://dx.doi.org/10.3390/ijms23179588

9. Olendzki B, Bucci V, Cawley C, Maserati R, McManus M, Olednzki E, et al. Dietary manipulation of the gut microbiome in inflammatory bowel disease patients: Pilot study. Gut Microbes. 2022 Jan-Dec;14(1):2046244.

Authors

Valentina Artusa, Ana Rita Franco, Prof. Francesco Peri
Department of Biotechnology and Biosciences, University Milano-Bicocca, Italy

Stefano Ceroni, Karin Böttcher, Véronique Berchet
Revvity

Revvity, Inc.
940 Winter Street
Waltham, MA 02451 USA
www.revvity.com

For a complete listing of our global offices, visit www.revvity.com